



Effect of substituents on the UV spectra of supermolecular system: Silver nanoparticles with bi-aryl Schiff bases containing hydroxyl

Chao-Tun Cao | Shimao Cheng | Jingyuan Zhang | Chenzhong Cao

Key Laboratory of Theoretical Organic Chemistry and Function Molecule, Ministry of Education, Key Laboratory of QSAR/QSPR of Hunan Provincial University, School of Chemistry and Chemical Engineering, Hunan University of Science and Technology, Xiangtan, China

Correspondence

Chenzhong Cao, Key Laboratory of Theoretical Organic Chemistry and Function Molecule, Ministry of Education, Key Laboratory of QSAR/QSPR of Hunan Provincial University, School of Chemistry and Chemical Engineering, Hunan University of Science and Technology, Xiangtan 411201, China.
Email: czcao@hnust.edu.cn

Funding information

National Nature Science Foundation of China, Grant/Award Number: 21672058

Abstract

Effect of substituents on the ultraviolet (UV) spectra of supermolecular system involving silver nanoparticles (AgNPs) and Schiff bases was investigated. AgNPs and 49 samples of model compounds (MC), bi-aryl Schiff bases containing hydroxyl (XBAY, involving 4-OHArCH=NArY, 2-OHArCH=NArY, XArCH=NAr-4'-OH, and XArCH=NAr-2'-OH), were synthesized. The size of AgNPs was characterized by transmission electron microscopy (TEM), and the UV absorption spectra of AgNPs, XBAYs, and MC-AgNPs mixed solutions were measured, respectively. The results show that (1) the size of AgNPs is larger in MC-AgNPs solutions than that in AgNPs solution due to the distribution of MC molecules on the surface of AgNPs; (2) the UV absorption wavelength of XBAYs changes in the action of AgNPs and their wavelength shift exists limitation between XBAY and MC-AgNPs solutions; and (3) the wavelength shift limit of MC-AgNPs (λ_{WSL}) is influenced by the substituents X and Y and the position of hydroxyl OH. The wavenumber $\Delta\nu_{\text{WSL}}$ of λ_{WSL} can be quantified by employing the excited-state substituent constant $\sigma_{\text{CC}}^{\text{ex}}$ and Hammett constant σ of substituents X and Y. Comparing with the 4-OH, the 4'-OH makes the $\Delta\nu_{\text{WSL}}$ a red shift, whereas the 2'-OH, comparing with the 2-OH, makes the $\Delta\nu_{\text{WSL}}$ a blue shift.

KEYWORDS

absorption wavelength shift, Schiff base, silver nanoparticles, substituent effect, ultraviolet absorption spectra

1 | INTRODUCTION

The optical properties of organic compounds can significantly change in the action of silver nanoparticles (AgNPs), such as enhancement of ultraviolet (UV) absorption and enhancement of Raman spectrum.^[1-6] However, it is still not clear how do the substituents affect the UV spectra of organic compounds in the action of AgNPs.

Previous researches showed that an organic compound with some functional groups such as hydroxyl

OH, amino NH₂, and mercapto SH could combine with AgNPs and changed its wavelength of UV absorption and intensity of Raman spectrum.^[1-21] For example, the AgNPs combining with mercapto SH of organic molecules were widely used to detect selectively glutathione,^[2] monitor the onset of surface screening effects of plasma resonance,^[4] promote the cysteine-functionalized AgNP aggregates,^[7] and investigate the photochromism of azobenzenes.^[9] The AgNPs combining with amino NH₂ of organic molecules were widely investigated. Gill

et al.^[3] studied on the simultaneous modification of fluorescence intensity and lifetime of dye-labeled DNA in the presence of aggregated AgNPs. Su et al.,^[13] Tang et al.,^[15] and Shahid et al.^[18] employed AgNPs for the ultrasensitive and multiplex DNA/miRNA detection, dyeing natural protein fibers and silk functionalization. Also, AgNPs received other applications, such as determination of low-activity hydrolases using Excited-State Intramolecular Proton-Transfer (ESIPT) fluorescent indicators on silver surfaces,^[14] applications of the optical properties of the silver clusters in the conformational studies of human telomeric DNA,^[17] and detection and removal of rhodamine dyes by AgNPs.^[1,6,10]

From the above reports, we think that if a series of compounds with various substituents has a specific functional group (eg, OH, NH₂, or SH), how do the UV spectra of these compounds change in the action of AgNPs. It is a very interesting topic. In this paper, we chose bi-aryl Schiff bases containing hydroxyl XArCH=NArY as model compounds to investigate the mentioned topic.

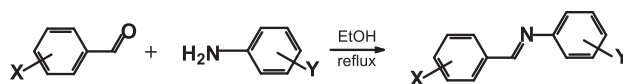
2 | EXPERIMENTAL SECTION

2.1 | Materials

Fish sperm DNA (fsDNA) was purchased from Boao Bio-Technology Co, Ltd (Shanghai, China). Silver nitrate (AgNO₃, 99%), sodium borohydride (NaBH₄, >98.0%), aromatic aldehydes (>98.0%), and aromatic amines (>98.0%) were purchased from J&K Scientific Ltd. All chemicals were of analytic grade and used as received without further purification.

2.2 | Preparation of AgNPs

In this work, 96 mL of fsDNA (1.0 g·L⁻¹), 4 mL of AgNO₃ (20.0mM) and 10 mL of NaBH₄ (2.0mM) were employed (total volume 110 mL) to prepare AgNPs solution according to Long's method,^[22,23] in which the fsDNA was used as template in order to avoid the aggregation of AgNPs. The final concentration of Ag is $c_{Ag} = 0.727\text{mM}$ in the AgNPs solution.



1, 2, 3, 4

1a - 1n: X=4-OH; Y = *p*-OMe, *p*-Me, *p*-H, *p*-F, *p*-Cl, *p*-Br, *p*-CF₃, *m*-OMe, *m*-Me, *m*-F, *m*-Cl, *m*-Br, *m*-CF₃, *m*-CN.

2a - 2m: X=2-OH; Y = *p*-OMe, *p*-Me, *p*-H, *p*-F, *p*-Cl, *p*-Br, *p*-CF₃, *p*-CN, *m*-F, *m*-Cl, *m*-Br, *m*-CF₃, *m*-CN.

3a - 3l: Y=4'-OH; X = *p*-NMe₂, *p*-OMe, *p*-Me, *p*-H, *p*-Cl, *p*-Br, *p*-CN, *m*-OMe, *m*-Me, *m*-F, *m*-Cl, *m*-Br.

4a - 4j: Y=2'-OH; X = *p*-OMe, *p*-Me, *p*-H, *p*-Cl, *p*-CN, *m*-F, *m*-Cl, *m*-Br, *m*-CF₃, *m*-CN.

2.3 | Preparation of model compounds

According to our previous reports,^[24-26] the substituted aryl Schiff bases containing ortho/para hydroxyl XArCH=NArY (XBAYs) were synthesized with the method as shown in Figure 1. These compounds were purified by recrystallization in anhydrous alcohol and were confirmed with ¹H NMR and ¹³C NMR. The NMR spectra were recorded with a Bruker AV 500 MHz spectrometer in DMSO (or CDCl₃). The detailed data of the synthesized compounds (2e, 2f, 2g, 2j, 3a, and 4a) are available in the Supporting Information.

2.4 | Measurement of UV absorption spectra

The model compounds XBAYs (MC) were vacuum dried for a whole day before measurement. The concentration of MC solution was 0.727mM, prepared by dissolving MC in anhydrous ethanol (total volume 10 mL). The MC solution and above AgNPs solution were employed to measure the UV spectra. All UV spectra of the MC solution, AgNPs solution, and MC-AgNPs mixed solution (supermolecular system) were recorded with a Shimadzu UV-2550 Spectrophotometer (Japan) at room temperature, scanning range 200 to 500 nm.

2.4.1 | UV spectra of model compounds

For each model compound, 50-μL MC solution was added into anhydrous ethanol in a sample cell (total volume 3 mL). Then the UV spectrum of MC solution was recorded. The peak of λ_{max} (nm) and the peak next to the λ_{max} (expressed by the symbol " λ'_{max} ") values were collected and converted into corresponding wavenumber ν_{max} (cm⁻¹, $\nu_{\text{max}} = 1/\lambda_{\text{max}}$) and ν'_{max} (cm⁻¹, $\nu'_{\text{max}} = 1/\lambda'_{\text{max}}$) values.

2.4.2 | UV spectrum of AgNPs solution

In a sample cell, 50-μL AgNPs solution was added into anhydrous ethanol (total volume 3 mL). Then the UV spectrum of AgNPs solution was recorded.

FIGURE 1 Synthesis of model compounds (1-4 XBAYs, bi-aryl Schiff bases containing hydroxyl OH)

2.4.3 | UV spectra of MC-AgNPs solutions

For each model compound, 50- μ L MC solution was mixed with $50 \times N$ μ L AgNPs solution to form the MC-AgNPs solutions in anhydrous ethanol in a sample cell (total volume 3 mL), where $N = 1, 2, 3, \dots$, indicating the molar ratio 1: N of MC versus Ag (counted with c_{Ag}). The MC-AgNPs solutions were kept on for 0.5 hour in avoiding light condition, and then their UV spectra were recorded. The $\lambda_{\text{max, mix}}$ and the next to $\lambda_{\text{max, mix}}$ (expressed by the symbol " $\lambda'_{\text{max, mix}}$ ") values of these MC-AgNPs solutions were collected and converted into corresponding $\nu_{\text{max, mix}}$ and $\nu'_{\text{max, mix}}$ values.

3 | RESULTS AND DISCUSSION

3.1 | Size change of AgNPs

The prepared AgNPs were characterized by transmission electron microscopy (TEM). Figure 2 showed the TEM and particle size distribution histogram, in which the average diameter of AgNPs was about 3.0 nm. In order to probe the size of AgNPs in MC-AgNPs solutions, we took **1b** (4-HOBA-Me-*p*) as an example. We added five times AgNPs solution (molar ratio) into **1b** (4-HOBA-Me-*p*) solution (forming **1b**-AgNPs mixed solution) and kept on stirring the mixed solution for 0.5 hour. Then we characterized the **1b**-AgNPs by TEM. Its TEM and particle size distribution histogram were showed in Figure 3. The average diameter of AgNPs in **1b**-AgNPs

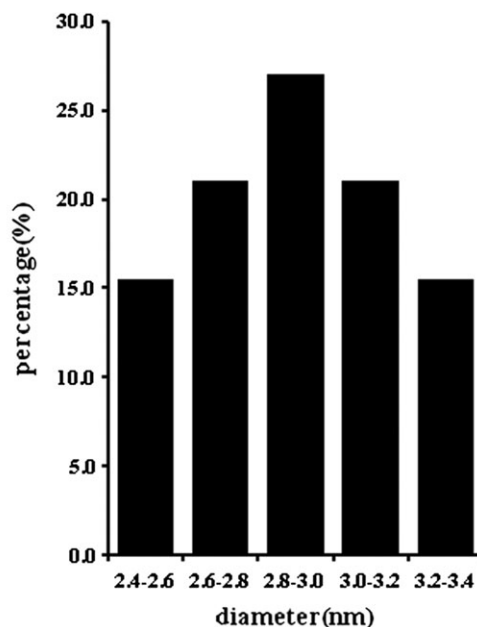
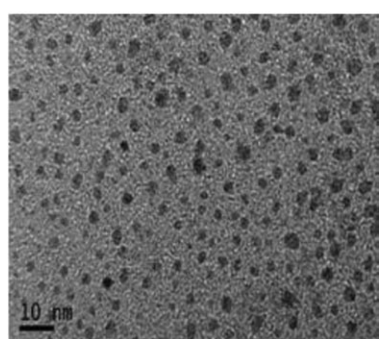


FIGURE 2 (left) Transmission electron microscopy and (right) particle size distribution diagram of silver nanoparticles (AgNPs) in AgNPs solution

was about 6.3 nm. Figures 2 and 3 show that the size of AgNPs in MC-AgNPs solution is larger than that of AgNPs in AgNPs solution. The size increase of AgNPs in MC-AgNPs may be due to the distribution of MC molecules on the surface of AgNPs. As regards the compound **1b**, its molecular length is about 1.3 nm in the crystal obtained by author (Scheme 1, CCDC No. 1868708; the checkCIF can be seen in the Supporting Information); thus, the average diameter of **1b**-AgNPs should be more than $3.0 + 2 \times 1.3 = 5.6$ nm. It is consistent with the measured results of Figure 3.

3.2 | UV spectra of MC and AgNPs solution

To observe the effect of concentration of MC and AgNPs on the UV spectra, we recorded the UV spectra of **1b** and AgNPs in different concentrations, respectively, as shown in Figure 4. It can be seen from Figure 4 that the UV absorption wavelengths of **1b** and AgNPs all do not change in the concentrations of 1.0×10^{-5} M to 10^{-4} M and only increase the absorbance as the concentrations raise. The λ_{max} of AgNPs is 263.4 nm (Figure 4, right).

3.3 | UV spectra of MC-AgNPs solutions

It was observed that, in the process of adding AgNPs into MC solution, the λ_{max} of XBAY did not change, whereas the $\lambda'_{\text{max, mix}}$ of XBAY was shifted. Take **1b**, for example; Figure 5 (left) showed that, in the **1b**-AgNPs (molar ratio

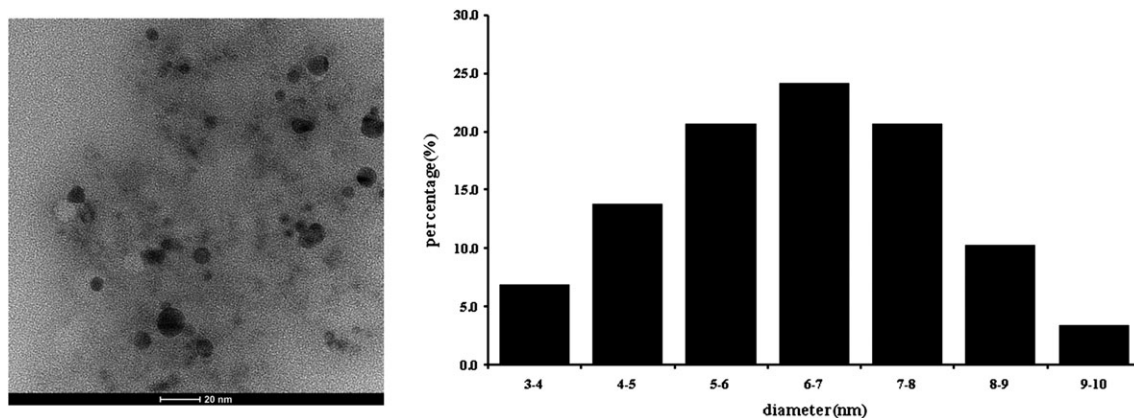
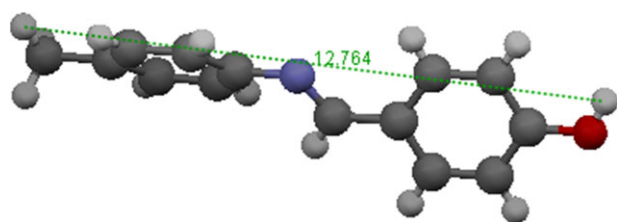


FIGURE 3 (left) Transmission electron microscopy and (right) particle size distribution diagram of silver nanoparticles (AgNPs) in **1b**-AgNPs mixed solution (molar ratio **1b**:Ag = 1:5)



SCHEME 1 The molecular conformation of **1b** in crystal (molecular length is about 1.3 nm)

5:2) solution, (1) the λ_{\max} of **1b** did not change (that is, the λ_{\max} of **1b** was equal to the $\lambda_{\max, \text{mix}}$ of **1b**-AgNPs) and only the absorbance of the λ_{\max} reduced, (2) whereas the λ'_{\max} of **1b** shifted ($\lambda'_{\max} > \lambda'_{\max, \text{mix}}$) and the absorbance of the λ'_{\max} increased and (3) the λ_{\max} of AgNPs solution disappeared. Figure 5 (right) showed that the $\lambda'_{\max, \text{mix}}$ of **1b**-AgNPs solution changed rapidly from the molar ratio of **1b**:Ag being 1:0 to 1:2. However, the $\lambda'_{\max, \text{mix}}$ did no longer change in case of the molar ratio of **1b**:Ag being more than 1:5. Thus, we take this $\lambda'_{\max, \text{mix}}$ as limit wavelength $\lambda'_{\max, \text{lim}}$ and take the wavelength interval between the λ'_{\max} of MC and the $\lambda'_{\max, \text{lim}}$ of MC-AgNPs solution as the wavelength shift limit of MC-AgNPs (λ_{WSL}), namely, $\lambda_{\text{WSL}} = \lambda'_{\max} - \lambda'_{\max, \text{lim}}$. For

example, the λ'_{\max} of **1b** is 292.8 nm, and the $\lambda'_{\max, \text{lim}}$ of **1b**-AgNPs is 264.6 nm; therefore, the $\lambda_{\text{WSL}} = \lambda'_{\max} - \lambda'_{\max, \text{lim}} = 292.8 - 264.6 = 28.2$ nm for the **1b**-AgNPs.

Since the $\lambda'_{\max, \text{mix}}$ of **1b**-AgNPs solutions shifts rapidly at the molar ratio of **1b**:Ag being from 1:0 to 1:2, we performed a detailed investigation for the $\lambda'_{\max, \text{mix}}$ change. The result was showed in Figure 6. In order to investigate whether Figure 6 is a peak of the simple sum of the λ_{\max} peak of AgNPs and the λ'_{\max} peak of MC or not, we added simply the UV spectra of AgNPs into that of **1b** by means of employing diverse molar ratios of **1b**:Ag and got their calculated UV spectra. Then, from the calculated UV spectra, we extracted the calculated $\lambda'_{\max, \text{mix}}$ peak. The experimental $\lambda'_{\max, \text{mix}}$ values of **1b**-AgNPs solutions and the calculated $\lambda'_{\max, \text{mix}}$ values of the simple sum of the AgNPs and **1b** were all presented in Figure 7.

Figure 6 indicates that the wavelength of $\lambda'_{\max, \text{mix}}$ changes continuously with the adding AgNPs into **1b** solution. Figure 7 shows that the wavelength of $\lambda'_{\max, \text{mix}}$ decreases rapidly at the beginning addition of AgNPs and then decreases slowly with the continuous adding AgNPs, and also, the experimental $\lambda'_{\max, \text{mix}}$ of **1b**-AgNPs

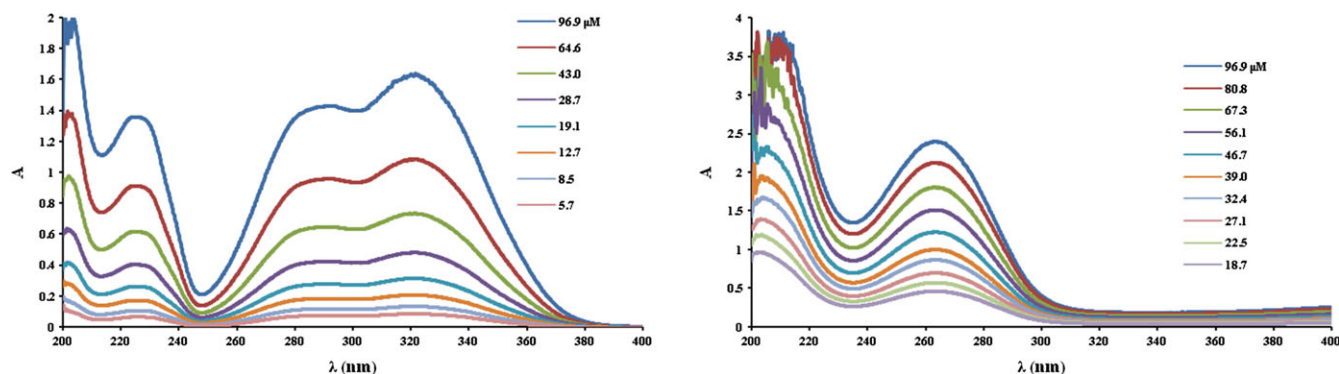


FIGURE 4 The UV absorption spectra of **1b** (left) and silver nanoparticles (AgNPs) (right) in different concentrations

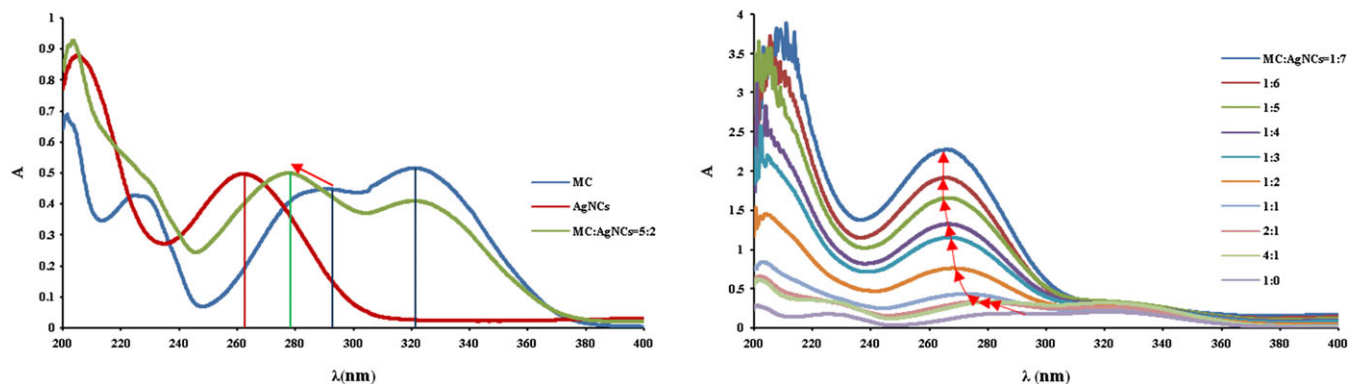


FIGURE 5 (left) The UV absorption spectra of **1b** (4-OHBA-Me-*p*), silver nanoparticles (AgNPs), and **1b**-AgNPs (5:2) solution, and (right) **1b**-AgNPs solution at different molar ratio of **1b**:Ag (bottom 1:0 to top 1:7)

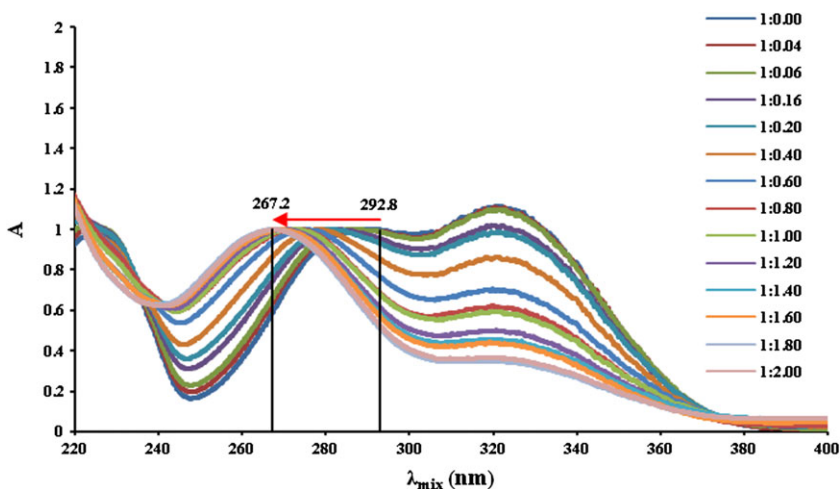


FIGURE 6 The wavelength shift process of **1b**-AgNPs solutions at equal absorbance (molar ratios of **1b**:Ag are 1:0 to 1:2). AgNPs, silver nanoparticles

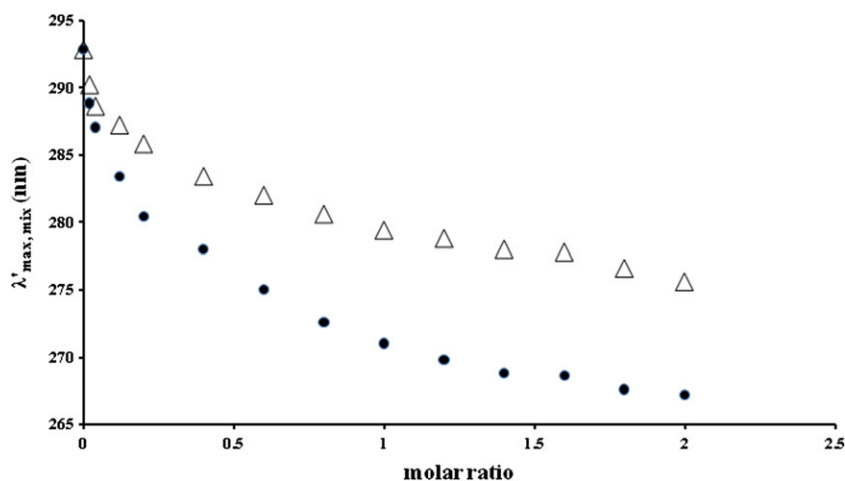


FIGURE 7 Plot of $\lambda'_{\text{max,mix}}$ versus the molar ratios of **1b**:Ag. (The \bullet indicates the experimental $\lambda'_{\text{max,mix}}$ of **1b**-AgNPs solutions; the Δ indicates the calculated $\lambda'_{\text{max,mix}}$ of simple sum of the AgNPs and **1b**). AgNPs, silver nanoparticles

decreases rapidly than the calculated $\lambda'_{\text{max,mix}}$ of the simple sum of the AgNPs and **1b**, which means that there is an interaction between MC molecules and AgNPs.

In this paper, 49 samples of MC solutions were employed to mix with the AgNPs solution at different

molar ratio and their limit wavelength $\lambda'_{\text{max,lim}}$ were recorded. Then their wavelength shift limits (λ_{WSL}) of MC-AgNPs solutions were obtained from the couples of λ'_{max} of MC and $\lambda'_{\text{max,lim}}$ of MC-AgNPs solution. The λ'_{max} of MC solution and λ_{WSL} of MC-AgNPs solution were

listed in Tables 1 and 2, respectively, in which the λ_{WSL} values were listed in descending order (large to small).

The wavelength changing from the λ'_{max} of MC solution to the $\lambda'_{\text{max, lim}}$ of MC-AgNPs solution may be due to the formation of aggregates between MC and AgNPs. According to the reports of literature,^[2,3,8,13,19,34] the surface of nanoparticles can be combined with O, S, and N atoms of organic molecules to form a nanoparticle whose surface links many organic molecules (that is, nanoparticle-organic molecule complexes, NOC). For these XBAY molecules used in this work, they have hydroxyl OH and bridging bond CH=N, and their O

and N atoms can combine with AgNPs. Perhaps, these interactions between MC molecules and AgNPs can be illustrated with Figure 8. Therefore, we assume that there are Nx free MC molecules in the original MC solution. After adding AgNPs into MC solution, each piece of AgNPs can adsorb x MC molecules on its surface to form an NOC, namely, AgNPs-MC _{x} . As the AgNPs are added continuously into the MC solution, the AgNPs-MC _{x} number increase gradually; thus, the free MC molecules in the solution decrease gradually, and at last, the AgNPs-MC _{x} solution forms. It can be expected that the $\lambda'_{\text{max, lim}}$ of MC-AgNPs solution should be the UV absorption

TABLE 1 The λ'_{max} (nm) of MC, λ_{WSL} (nm) of MC-AgNPs, $\Delta\nu_{\text{WSL}}$ (cm⁻¹), and substituent effect constants of groups X and Y for XBAYs (1 and 3)

No.	Compound	λ'_{max}	λ_{WSL}	$\Delta\nu_{\text{WSL}}^{\text{a}}$	$\sigma(\text{X})^{\text{b}}$	$\sigma(\text{Y})^{\text{b}}$	$\sigma_{\text{CC}}^{\text{ex}}(\text{X})^{\text{c}}$	$\sigma_{\text{CC}}^{\text{ex}}(\text{Y})^{\text{c}}$	$I_{(4'-\text{OH})}^{\text{d}}$
1h	4-HOBA-OMe- <i>m</i>	294.4	30.8	-3969	-0.37	0.12	-0.19	0.10	0
1i	4-HOBA-Me- <i>m</i>	294.4	30.8	-3969	-0.37	-0.07	-0.19	-0.03	0
1c	4-HOBA-H- <i>p</i>	294.8	29.6	-3786	-0.37	0.00	-0.19	0.00	0
1g	4-HOBA-CF ₃ - <i>p</i>	292.2	29.4	-3829	-0.37	0.54	-0.19	-0.12	0
1j	4-HOBA-F- <i>m</i>	295.0	29.2	-3724	-0.37	0.34	-0.19	0.02	0
1m	4-HOBA-CF ₃ - <i>m</i>	294.0	29.0	-3722	-0.37	0.43	-0.19	0.09	0
1n	4-HOBA-CN- <i>m</i>	292.8	28.6	-3697	-0.37	0.56	-0.19	0.56	0
1b	4-HOBA-Me- <i>p</i>	292.8	28.2	-3640	-0.37	-0.17	-0.19	-0.17	0
1l	4-HOBA-Br- <i>m</i>	290.6	25.6	-3324	-0.37	0.39	-0.19	-0.03	0
1f	4-HOBA-Br- <i>p</i>	287.0	23.4	-3093	-0.37	0.23	-0.19	-0.33	0
1e	4-HOBA-Cl- <i>p</i>	286.6	22.6	-2987	-0.37	0.23	-0.19	-0.22	0
1a	4-HOBA-OMe- <i>p</i>	287.2	22.6	-2974	-0.37	-0.27	-0.19	-0.50	0
1d	4-HOBA-F- <i>p</i>	286.8	21.8	-2868	-0.37	0.06	-0.19	0.06	0
1k	4-HOBA-Cl- <i>m</i>	285.6	21.4	-2836	-0.37	0.37	-0.19	0.02	0
3a	<i>p</i> -NMe ₂ BA-4'-OH	297.6	36.2	-4639	-0.83	-0.37	-1.81	-0.19	1
3b	<i>p</i> -OMeBA-4'-OH	281.2	15.6	-2089	-0.27	-0.37	-0.50	-0.19	1
3g	<i>p</i> -CNBA-4'-OH	276.2	15.6	-2167	0.66	-0.37	-0.70	-0.19	1
3f	<i>p</i> -BrBA-4'-OH	272.4	10.4	-1457	0.23	-0.37	-0.33	-0.19	1
3l	<i>m</i> -BrBA-4'-OH	268.8	8.2	-1171	0.39	-0.37	-0.03	-0.19	1
3e	<i>p</i> -ClBA-4'-OH	269.4	8.0	-1136	0.23	-0.37	-0.22	-0.19	1
3h	<i>m</i> -OMeBA-4'-OH	268.4	7.8	-1115	0.12	-0.37	0.10	-0.19	1
3i	<i>m</i> -MeBA-4'-OH	267.2	7.0	-1007	-0.07	-0.37	-0.03	-0.19	1
3c	<i>p</i> -MeBA-4'-OH	269.8	6.8	-958	-0.17	-0.37	-0.17	-0.19	1
3j	<i>m</i> -FBA-4'-OH	266.4	6.0	-865	0.34	-0.37	0.02	-0.19	1
3k	<i>m</i> -ClBA-4'-OH	266.6	5.4	-775	0.37	-0.37	0.02	-0.19	1
3d	<i>p</i> -HBA-4'-OH	264.4	3.6	-522	0.00	-0.37	0.00	-0.19	1

^a $\Delta\nu_{\text{WSL}} = 1/\lambda'_{\text{max}} - 1/\lambda'_{\text{max, lim}}$.

^bThe values were taken from Hansh et al.^[27]

^cThe values were taken from previous studies.^[28-33]

^dIndicator variable of 4'-OH.

TABLE 2 The λ'_{\max} (nm) of MC, λ_{WSL} (nm) of MC-AgNPs, $\Delta\nu_{\text{WSL}}$ (cm^{-1}), and substituent effect constants of groups X and Y for XBAYs (2 and 4)

No.	Compound	λ'_{\max}	λ_{WSL}	$\Delta\nu_{\text{WSL}}^{\text{a}}$	$\sigma(\text{X})^{\text{b}}$	$\sigma(\text{Y})^{\text{b}}$	$\sigma_{\text{CC}}^{\text{ex}}(\text{X})^{\text{c}}$	$\sigma_{\text{CC}}^{\text{ex}}(\text{Y})^{\text{c}}$	$I_{(2'-\text{OH})}^{\text{d}}$
2h	2-HOBA-CN- <i>p</i>	280.2	14.8	-1990	-0.38	0.66	-0.10	-0.70	0
2g	2-HOBA-CF ₃ - <i>p</i>	271.6	11.4	-1613	-0.38	0.54	-0.10	-0.12	0
2m	2-HOBA-CN- <i>m</i>	274.2	10.0	-1380	-0.38	0.56	-0.10	0.56	0
2k	2-HOBA-Br- <i>m</i>	271.6	8.4	-1175	-0.38	0.39	-0.10	-0.03	0
2e	2-HOBA-Cl- <i>p</i>	271.2	8.2	-1150	-0.38	0.23	-0.10	-0.22	0
2i	2-HOBA-F- <i>m</i>	271.6	8.0	-1117	-0.38	0.34	-0.10	0.02	0
2f	2-HOBA-Br- <i>p</i>	269.6	7.8	-1105	-0.38	0.23	-0.10	-0.33	0
2l	2-HOBA-CF ₃ - <i>m</i>	271.4	7.6	-1062	-0.38	0.43	-0.10	0.09	0
2a	2-HOBA-OCH ₃ - <i>p</i>	270.6	6.6	-924	-0.38	-0.27	-0.10	-0.50	0
2j	2-HOBA-Cl- <i>m</i>	270.6	6.6	-924	-0.38	0.37	-0.10	0.02	0
2c	2-HOBA-H- <i>p</i>	268.8	5.8	-820	-0.38	0.00	-0.10	0.00	0
2d	2-HOBA-F- <i>p</i>	269.8	5.6	-786	-0.38	0.06	-0.10	0.06	0
2b	2-HOBA-CH ₃ - <i>p</i>	268.8	5.0	-705	-0.38	-0.17	-0.10	-0.17	0
4a	<i>p</i> -OMe-BA-2'-OH	285.2	19.6	-2587	-0.27	-0.38	-0.50	-0.10	1
4e	<i>p</i> -CN-BA-2'-OH	276.2	15.8	-2197	0.66	-0.38	-0.70	-0.10	1
4d	<i>p</i> -Cl-BA-2'-OH	269.4	8.2	-1165	0.23	-0.38	-0.22	-0.10	1
4b	<i>p</i> -Me-BA-2'-OH	269.8	7.6	-1074	-0.17	-0.38	-0.17	-0.10	1
4c	<i>p</i> -H-BA-2'-OH	263.0	2.4	-350	0.00	-0.38	0.00	-0.10	1
4h	<i>m</i> -Br-BA-2'-OH	264.0	2.0	-289	0.39	-0.38	-0.03	-0.10	1
4g	<i>m</i> -Cl-BA2'-OH	264.0	1.2	-173	0.37	-0.38	0.02	-0.10	1
4f	<i>m</i> -F-BA-2'-OH	260.6	-1.0	147	0.34	-0.38	0.02	-0.10	1
4i	<i>m</i> -CF ₃ -BA-2'-OH	261.8	-1.4	203	0.43	-0.38	0.09	-0.10	1
4j	<i>m</i> -CN-BA-2'-OH	257.6	-5.4	797	0.56	-0.38	0.56	-0.10	1

^a $\Delta\nu_{\text{WSL}} = 1/\lambda'_{\max} - 1/\lambda_{\max, \text{lim}}$.

^bThe values were taken from Hansh et al.^[27]

^cThe values were taken from previous studies.^[28-33]

^dIndicator variable of 2'-OH.

wavelength of AgNPs-MC_x (neither the λ'_{\max} of XBAY nor the λ_{\max} of AgNPs), which is close to but not equal to the λ_{\max} of AgNPs (263.4 nm). In fact, the experimental $\lambda'_{\max, \text{lim}}$ of MC-AgNPs solutions in Tables 1 and 2 are all in the range of 260.0 to 266.0 nm, which coincide with the above expectations.

The λ_{WSL} values of Tables 1 and 2 show that, on the whole, the λ_{WSL} values of **1** and **3** (containing 4/4'-OH) are larger than that of **2** and **4** (containing 2/2'-OH). In the series of compounds **1** and **3**, the most λ_{WSL} value is of **3a** (*p*-NMe₂BA-OH-4'), up to 36.2 (nm). It should be noted that the positive λ_{WSL} value indicates a blue shift and negative λ_{WSL} value is a red shift. In Tables 1 and 2, some of the MC-AgNPs solutions have larger λ_{WSL} value and the others have smaller λ_{WSL} value. Some of the MC-AgNPs solutions have wavelength blue shift, and the

others have wavelength red shift. Figures 9 and 10 indicate the change of λ_{WSL} values. These λ_{WSL} values are dominated by the location of hydroxyl OH and the type of substituents in MC molecules.

3.4 | Effect of substituent on the wavelength shift limit λ_{WSL}

To quantify the effect of substituent on the UV spectra of organic compounds, author's group^[28-33] proposed excited-state substituent constant $\sigma_{\text{CC}}^{\text{ex}}$. Using the $\sigma_{\text{CC}}^{\text{ex}}$ constant together with Hammett electronic effect constant σ ,^[27] the wavenumbers ν_{\max} of the λ_{\max} were well correlated for these conjugated compounds involving substituted stilbenes and benzenes,^[25,30-33,35-38] styrene

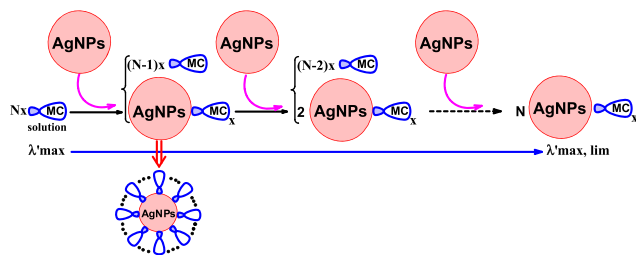


FIGURE 8 Diagram of MC molecules interacting with silver nanoparticles (AgNPs) in the process of adding AgNPs into MC solution (where Nx , $(N-1)x$, $(N-2)x$, ..., and N are the number of free MC molecules and x is the number of MC molecules distributing on the surface of AgNPs)

derivatives,^[28,32] aryl Schiff bases,^[39–52] and disubstituted pyrimidines.^[53] Here, we also employed the excited-state substituent constant σ_{CC}^{ex} and Hammett electronic effect constant σ to quantify the $\Delta\nu_{WSL}$ of MC-AgNPs solutions. After optimizing, we obtained the regression equation (1) and equation (2), respectively.

For the XBAYs (1 and 3)-AgNPs,

$$\begin{aligned} \Delta\nu_{WSL} = & -2574.05 + 1327.857\sigma_R(X) \\ & + 1975.339\sigma_F(Y) \\ & + 1387.344\sigma_{CC}^{ex}(X) - 550.787\sigma_{CC}^{ex}(Y) - 722.466\Delta\sigma^2 \\ & + 1233.244I_{(4'-OH)} \\ R = & 0.9845, S = 256.8, F = 99.87, n = 26 \end{aligned} \quad (1)$$

For the XBAYs (2 and 4)-AgNPs,

$$\begin{aligned} \Delta\nu_{WSL} = & 334.8966 + 1834.212\sigma(X) \\ & + 2666.438\sigma_{CC}^{ex}(X) \\ & + 423.5608\sigma_{CC}^{ex}(Y) - 794.64\Delta\sigma^2 - 907.115\Delta(\sigma_{CC}^{ex})^2 \\ & - 696.894I_{(2'-OH)} \\ R = & 0.9812, S = 175.7, F = 68.78, n = 23 \end{aligned} \quad (2)$$

where R is the correlation coefficient, S is the standard deviation, F is the Fisher ratio, and n is the data points of the regression equation, respectively.

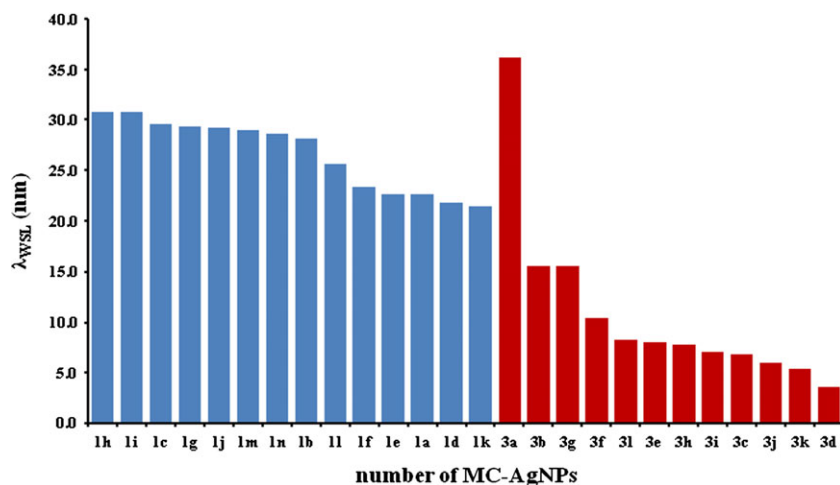


FIGURE 9 The λ_{WSL} value of XBAYs (1 and 3)-AgNPs mixed solutions (the number of MC is in Table 1). AgNPs, silver nanoparticles

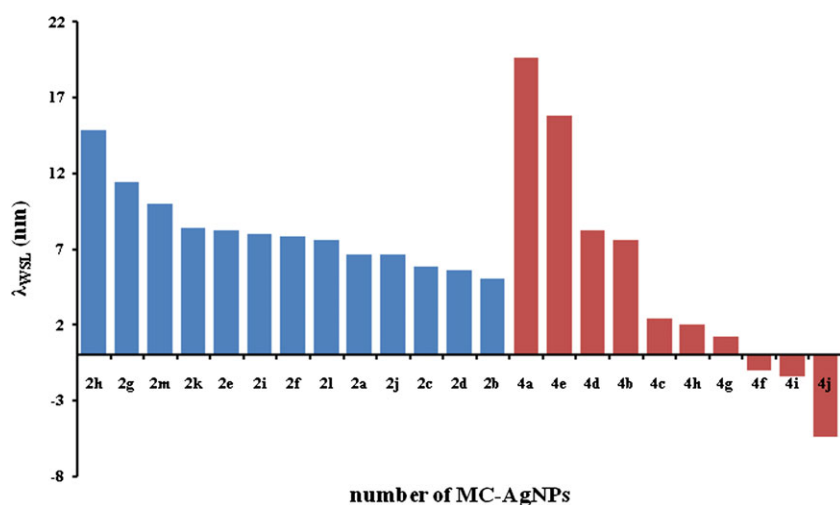


FIGURE 10 The λ_{WSL} value of XBAYs (2 and 4)-AgNPs mixed solutions (the number of MC is in Table 2). AgNPs, silver nanoparticles

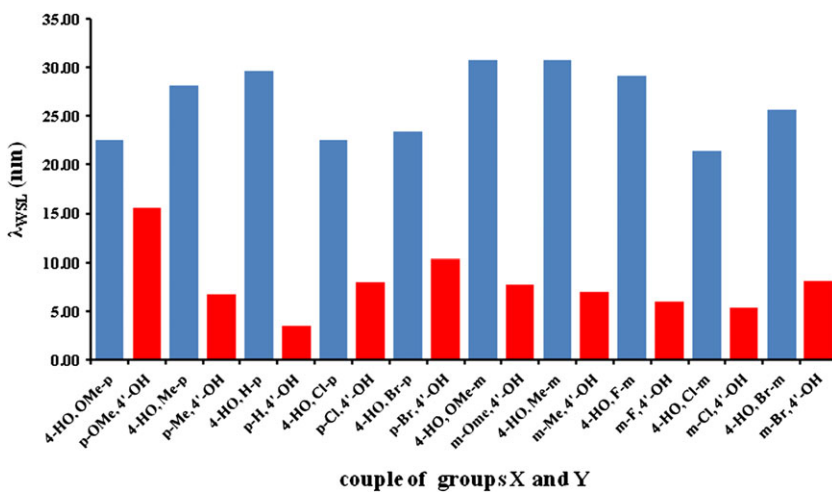


FIGURE 11 The λ_{WSL} (nm) of **1** (blue) and **3** (red) for the couples of X and Y (X = Y)

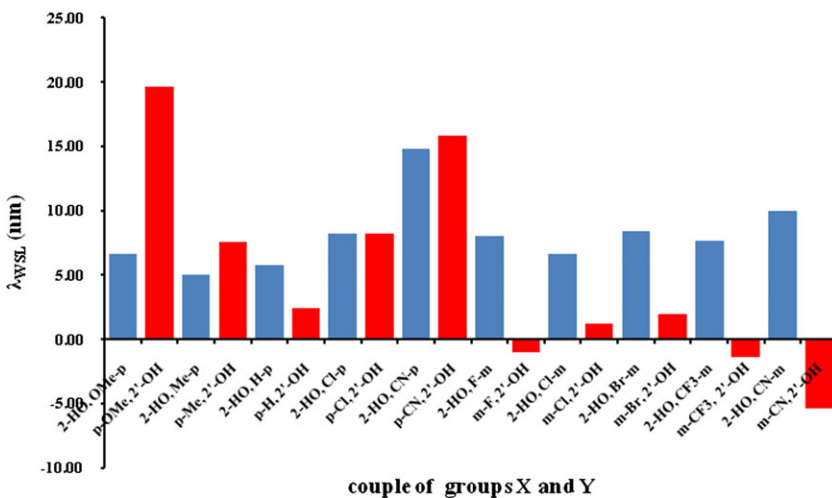


FIGURE 12 The λ_{WSL} (nm) of **2** (blue) and **4** (red) for the couples of X and Y (X = Y)

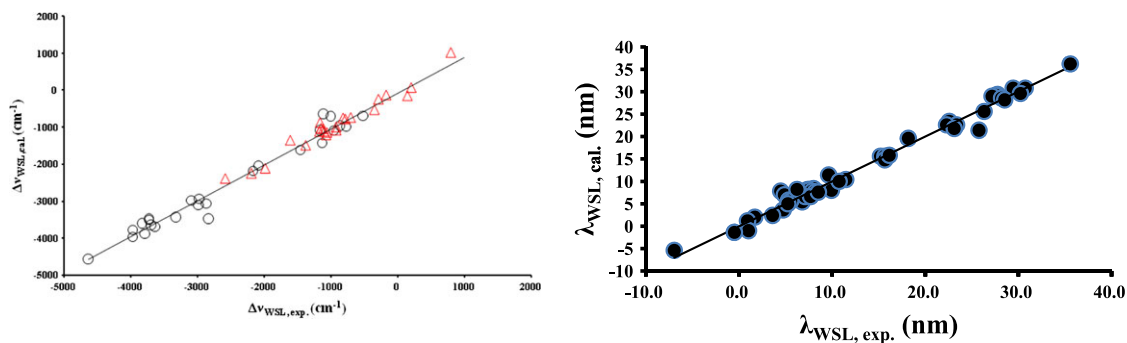


FIGURE 13 (left) Plot of calculated $\Delta\nu_{\text{WSL, cal}}$ versus experimental $\Delta\nu_{\text{WSL, exp}}$ of MC-silver nanoparticles (AgNPs) solutions for the XBAYs in Table 1 (O) and Table 2 (Δ) and (right) plot of calculated $\lambda_{\text{WSL, cal}}$ versus experimental $\lambda_{\text{WSL, exp}}$ of MC-AgNPs solutions for the XBAYs in Tables 1 and 2

In Equations 1 and 2, the meanings of parameters are as follows:

The σ is Hammett electronic effect constant of X or Y substituent in molecule XBAY; the $\sigma(X)$ and $\sigma(Y)$ indicate the σ value of X and Y, respectively; the σ_F and σ_R stand for the field/inductive effect and resonance effect, respectively, where $\sigma_F + \sigma_R = \sigma$ for the interested group X (or Y). The $\Delta\sigma^2$ is the substituent specific cross-interaction effect expressed with Hammett constant σ between X and Y, that is, $\Delta\sigma^2 = [\sigma(X) - \sigma(Y)]^2$.

The σ_{CC}^{ex} is the excited-state substituent constant of X or Y substituent in molecule XBAY; the $\sigma_{CC}^{ex}(X)$ and $\sigma_{CC}^{ex}(Y)$ indicate the σ_{CC}^{ex} value of X and Y, respectively.

The $\Delta(\sigma_{CC}^{ex})^2$ is the substituent specific cross-interaction effect expressed with excited-state substituent constant σ_{CC}^{ex} between X and Y, that is, $\Delta(\sigma_{CC}^{ex})^2 = [\sigma_{CC}^{ex}(X) - \sigma_{CC}^{ex}(Y)]^2$.

The $I_{(4'-OH)}$ is the indicator variable, when the molecule contains 4'-OH, $I_{4'-OH} = 1$, otherwise, $I_{4'-OH} = 0$.

The $I_{(2'-OH)}$ is the indicator variable, when the molecule contains 2'-OH, $I_{2'-OH} = 1$, otherwise, $I_{2'-OH} = 0$.

The results of Equations 1 and 2 show that the $\Delta\nu_{WSL}$ of MC-AgNPs solutions can be quantified by employing the excited-state substituent constant σ_{CC}^{ex} and Hammett electronic effect constant σ of substituents X and Y. However, there are some difference of the factors affecting the $\Delta\nu_{WSL}$ of MC-AgNPs solutions for the XBAYs containing 4/4'-OH (**1** and **3**) versus those containing 2/2'-OH (**2** and **4**). It can be seen from the coefficients in front of the parameters of Equations 1 and 2 that (1) the positive $\sigma_R(X)$, $\sigma_F(Y)$, and $\sigma_{CC}^{ex}(X)$ result in a red shift of $\Delta\nu_{WSL}$, and the positive $\sigma_{CC}^{ex}(Y)$ and $\Delta\sigma^2$ result in a blue shift of $\Delta\nu_{WSL}$ for the **1** and **3** XBAYs and (2) the positive $\sigma(X)$, $\sigma_{CC}^{ex}(X)$, and $\sigma_{CC}^{ex}(Y)$ result in a red shift of $\Delta\nu_{WSL}$, and the positive $\Delta\sigma^2$ and $\Delta(\sigma_{CC}^{ex})^2$ result in a blue shift of $\Delta\nu_{WSL}$ for the **2** and **4** XBAYs. In the solutions of (**1** and **3**)-AgNPs, the effect of $\Delta(\sigma_{CC}^{ex})^2$ on the $\Delta\nu_{WSL}$ can be ignored, whereas the effect of $\sigma(Y)$ on the $\Delta\nu_{WSL}$ can be ignored in the solutions of (**2** and **4**)-AgNPs. In addition, the coefficients in front of the indicator variables show that the effect of 4'-OH on the $\Delta\nu_{WSL}$ is different from that of 4-OH; also, the effect of 2'-OH on the $\Delta\nu_{WSL}$ is different from that of 2-OH. That

is, comparing with the 4-OH, the 4'-OH results in a red shift of $\Delta\nu_{WSL}$, whereas, comparing with the 2-OH, the 2'-OH results in a blue shift of $\Delta\nu_{WSL}$.

As regards the effect of position of X or Y group on the λ_{WSL} of XBAYs, there are two kinds of cases: One is the series of **1** and **3**, and the other is the series of **2** and **4**. In the former case, the compounds **1** have larger λ_{WSL} than **3** in case of substituent $X(m/p) = Y(m/p)$, as shown in Figure 11, whereas in the latter, the compounds **2** have generally smaller λ_{WSL} than **4** in case of $X(p) = Y(p)$, and in contrast, the compounds **2** have larger λ_{WSL} than **4** in case of $X(m) = Y(m)$, as shown in Figure 12.

Figure 13 is the plot of calculated $\Delta\nu_{WSL, cal}$ and $\lambda_{WSL, cal}$ with Equations 1 and 2 versus the experimental $\Delta\nu_{WSL, exp}$ and $\lambda_{WSL, exp}$ of Tables 1 and 2, respectively, which shows that the calculated $\Delta\nu_{WSL, cal}$ and $\lambda_{WSL, cal}$ values are in agreement with the experimental $\Delta\nu_{WSL, exp}$ and $\lambda_{WSL, exp}$ ones.

4 | CONCLUSION

Experimental results show that the UV absorption wavelength of bi-aryl Schiff bases containing hydroxyl (4/4'-OH and 2/2'-OH) changes in the action of AgNPs. The absorption wavelength exists a limitation, and these wavelength shift limits (λ_{WSL}) of MC-AgNPs solutions (supermolecular system) are influenced by substituents X and Y and the position of the hydroxyl OH. The wavenumber $\Delta\nu_{WSL}$ of wavelength shift limit can be quantified by employing the excited-state substituent constant σ_{CC}^{ex} and Hammett electronic effect constant σ of X and Y substituents. Comparing with the 4-OH, the 4'-OH makes the $\Delta\nu_{WSL}$ a red shift, and comparing with the 2-OH, the 2'-OH makes the $\Delta\nu_{WSL}$ a blue shift.

In addition, we also observed that bi-aryl Schiff bases without hydroxyl had different UV absorption behavior in the action of AgNPs. We will report these results in our subsequent paper.

ACKNOWLEDGEMENT

The work was supported by the National Nature Science Foundation of China (21672058).

ORCID

Chenzhong Cao  <http://orcid.org/0000-0001-5224-7716>

REFERENCES

- [1] S. Pan, Z. Wang, L. J. Rothberg, *J. Phys. Chem. B* **2006**, *110*, 17383.

- [2] Y. Bu, G. Zhu, S. Li, R. Qi, G. Bhavé, D. Zhang, R. Han, D. Sun, X. Liu, Z. Hu, X. Liu, *ACS Appl. Nano. Mater.* **2018**, *1*, 410.
- [3] R. Gill, L. Tian, W. R. C. Somerville, E. C. L., *J. Phys. Chem. C* **2012**, *116*, 16687.
- [4] K. B. Mogensen, K. Kneipp, *J. Phys. Chem. C* **2014**, *118*, 28075.
- [5] S. J. Bae, C.-r. Lee, I. S. Choi, C.-S. Hwang, M. Gong, K. Kim, S.-W. Joo, *J. Phys. Chem. B* **2002**, *106*, 7076.
- [6] J. M. Baik, S. J. Lee, *Nano Lett.* **2009**, *9*, 672.
- [7] M. Csete, A. Szalai, E. Csapó, L. Tóth, A. Somogyi, I. Dékány, *J. Phys. Chem. C* **2014**, *118*, 17940.
- [8] O.-M. Gui, S. C. Pinzaru, *Dyes Pigm.* **2017**, *146*, 551.
- [9] J.-J. Lin, W.-C. Lin, S.-D. Li, C.-Y. Lin, S.-h. Hsu, *ACS Appl. Mater. Interfaces* **2013**, *5*, 433.
- [10] J. Pang, Y. Chao, H. Chang, H. Li, J. Xiong, Q. Zhang, G. Chen, J. Qian, W. Zhu, H. Li, *Chem. Eng.* **2018**, *6*, 4948.
- [11] R. Sekine, K. L. Moore, M. Matzke, P. Vallotton, H. Jiang, G. M. Hughes, J. K. Kirby, E. Donner, C. R. M. Grovenor, C. Svendsen, E. Lombi, *ACS Nano* **2017**, *11*, 10894.
- [12] F. Taherkhani, S. Kiani, *J. Phys. Chem. C* **2017**, *121*, 24434.
- [13] J. Su, D. Wang, L. Nörbel, J. Shen, Z. Zhao, Y. Dou, T. Peng, J. Shi, S. Mathur, C. Fan, S. Song, *Anal. Chem.* **2017**, *89*, 2531.
- [14] I. E. Serdiuk, M. Reszka, A. Synak, B. Liberek, P. Bojarski, *Dyes Pigm.* **2018**, *149*, 224.
- [15] B. Tang, Y. Yao, W. Chen, X. Chen, F. Zou, X. Wang, *Dyes Pigm.* **2017**, *148*, 224.
- [16] D. M. Mitrano, E. Rimmele, A. Wichser, R. Erni, M. Height, B. Nowack, *ACS Nano* **2014**, *8*, 7208.
- [17] H.-C. Hsu, Y.-X. Lin, C.-W. Chang, *Dyes Pigm.* **2017**, *146*, 420.
- [18] M. Shahid, X.-W. Cheng, R.-C. Tang, G. Chen, *Dyes Pigm.* **2017**, *137*, 277.
- [19] N. O. Mahmoodi, A. Ghavidast, S. Mirkhaef, M. A. Zanjanchi, *Dyes Pigm.* **2015**, *118*, 110.
- [20] B. Tang, L. Sun, J. Li, J. Kaur, H. Zhu, S. Qin, Y. Yao, W. Chen, X. Wang, *Dyes Pigm.* **2015**, *113*, 289.
- [21] M. Blosi, S. Albonetti, F. Gatti, G. Baldi, M. M. Dondi, *Dyes Pigm.* **2012**, *94*, 355. <https://doi.org/10.1016/j.dyepig.2012.01.006>
- [22] S. Liang, Y. Kuang, F. Ma, S. Chen, Y. Long, *Biosens. Bioelectron.* **2016**, *85*, 758.
- [23] Y. Kuang, S. Liang, F. Ma, S. Chen, Y. Long, R. Zeng, *Luminescence* **2017**, *32*, 674.
- [24] C. Cao, B. Lu, G. Chen, *J. Phys. Org. Chem.* **2011**, *24*, 335.
- [25] L.-Y. Wang, C.-T. Cao, C.-Z. Cao, J. Chin, *Chem. Phys.* **2016**, *29*, 260.
- [26] L. Wang, C.-T. Cao, C. Cao, *J. Phys. Org. Chem.* **2016**, *29*, 299.
- [27] C. Hansh, A. Leo, R. W. Taft, *Chem. Rev.* **1991**, *91*, 165.
- [28] J. Qu, C.-T. Cao, C. Cao, *J. Phys. Org. Chem.* **2018**, *31*, e3799. <https://doi.org/10.1002/poc.3799>.
- [29] C.-T. Cao, W. Zhou, C. Cao, *J. Phys. Org. Chem.* **2017**, *30*, e3672. <https://doi.org/10.1002/poc.3672>
- [30] C. Cao, Y. Wu, *Sci. China Chem.* **2013**, *56*, 883.
- [31] C. Cao, B. Sheng, G. Chen, *J. Phys. Org. Chem.* **2012**, *25*, 1315.
- [32] C. Cao, G. Chen, Z. Yin, *J. Phys. Org. Chem.* **2008**, *21*, 808.
- [33] Q. Zhu, C.-T. Cao, C.-Z. Cao, *Acta Phys.-Chim. Sin.* **2017**, *33*, 729.
- [34] A. Wang, W. Sun, C. Wang, M. Xu, X. Lu, X. Tian, S. Li, J. Wu, Y. Tian, *Dyes Pigm.* **2017**, *141*, 13.
- [35] C. Cao, G. Chen, Y. Wu, *Sci. China Ser. B-Chem.* **2011**, *54*, 1735.
- [36] C. Cao, Y. Zhu, G. Chen, *J. Phys. Org. Chem.* **2013**, *26*, 834.
- [37] Y. Zhang, C.-T. Cao, J. Zhang, C. Cao, *J. Phys. Org. Chem.* **2017**, *30*, e3705. <https://doi.org/10.1002/poc.3705>
- [38] G. Chen, C. Cao, *J. Phys. Org. Chem.* **2010**, *23*, 776.
- [39] Z. Fang, F. Wu, B. Yi, C. Cao, X. Xin, *J. Mol. Struct.* **2016**, *1104*, 57.
- [40] C.-T. Cao, Y. Bi, C. Cao, *Spectrochim. Acta A* **2016**, *163*, 101.
- [41] Q. Luo, C.-T. Cao, Z. Cao, C. Cao, *J. Phys. Org. Chem.* **2016**, *29*, 406.
- [42] Z. Cao, C.-T. Cao, C. Cao, *J. Phys. Org. Chem.* **2015**, *28*, 564.
- [43] Q.-Q. Luo, C.-T. Cao, C.-Z. Cao, *Acta Phys.-Chim. Sin.* **2016**, *32*, 1691.
- [44] L. Wang, C.-T. Cao, C. Cao, *J. Phys. Org. Chem.* **2014**, *27*, 818.
- [45] Z. Fang, C. Cao, J. Chen, X. Deng, *J. Mol. Struct.* **2014**, *1063*, 307.
- [46] C. Cao, Z. Fang, *Spectrochim. Acta A* **2013**, *111*, 62.
- [47] Z. Fang, C. Cao, *J. Mol. Struct.* **2013**, *1036*, 447.
- [48] Y.-x. Wu, C.-z. Cao, Y. Yuan, *Chin. J. Chem. Phys.* **2012**, *25*(2), 153.
- [49] G. Chen, C. Cao, B. Lu, B. Sheng, *J. Phys. Org. Chem.* **2012**, *25*, 327.
- [50] C.-T. Cao, B.-Y. Wei, C.-Z. Cao, *Acta Phys.-Chim. Sin.* **2015**, *31*, 204.
- [51] C.-t. Cao, L. Wang, C. Cao, *Chin. J. Chem. Phys.* **2018**, *31*, 45.
- [52] C. Cao, Y. Bi, C.-T. Cao, J. Chin, *Org. Chem.* **2015**, *35*, 1302.
- [53] H. Yuan, M.-Y. Li, C.-N. Chen, Y. Zhang, W.-Q. Liu, *J. Phys. Org. Chem.* **2018**, e3860. <https://doi.org/10.1002/poc.3860>, 31.

SUPPORTING INFORMATION

Additional supporting information may be found online in the Supporting Information section at the end of the article.

How to cite this article: Cao C-T, Cheng S, Zhang J, Cao C. Effect of substituents on the UV spectra of supermolecular system: Silver nanoparticles with bi-aryl Schiff bases containing hydroxyl. *J Phys Org Chem.* 2018;e3910. <https://doi.org/10.1002/poc.3910>